

# Rheology of vesicle suspensions under combined steady and oscillating shear flows

A. Farutin<sup>†</sup> and C. Misbah

Université Grenoble 1/CNRS, Laboratoire Interdisciplinaire de Physique/UMR5588,  
Grenoble F-38041, France

(Received 28 July 2011; revised 22 December 2011; accepted 6 March 2012;  
first published online 30 April 2012)

Viscoelastic properties of complex fluids are usually extracted by applying an oscillatory shear rate ( $\dot{\gamma} = \alpha \dot{\gamma}_0 \cos(\omega t)$ , where  $\alpha \dot{\gamma}_0$  is a constant which is small for a linear response to make sense) to the fluid. This leads to a complex effective viscosity where its real part carries information on viscous effects while its imaginary part informs us on elastic properties. We show here theoretically, by taking a dilute vesicle suspension as an example, that application of a pure shearing oscillation misses several interesting microscopic features of the suspension. It is shown that if, in addition to the oscillatory part, a basic constant shear rate is applied to the suspension (so that the total shear rate is  $\dot{\gamma} = \dot{\gamma}_0(1 + \alpha \cos \omega t)$ , with  $\dot{\gamma}_0$  a constant), then the complex viscosity reveals much more insightful properties of the suspension. First, it is found that the complex viscosity exhibits a resonance for tank-treading vesicles as a function of the frequency of oscillation. This resonance is linked to the fact that vesicles, while being in the stable tank-treading regime (with their main axis having a steady orientation with respect to the flow direction), possess damped oscillatory modes. Second, in the region of parameter space where the vesicle exhibits either vacillating-breathing (permanent oscillations of the main axis about the flow direction and breathing of the shape) or tumbling modes, the complex viscosity shows an infinite number of resonances as a function of the frequency. It is shown that these behaviours markedly differ from that obtained when only the classical oscillation  $\dot{\gamma} = \alpha \dot{\gamma}_0 \cos(\omega t)$  is applied. The results are obtained numerically by solution of the analytical constitutive equation of a dilute vesicle suspension and confirmed analytically by a linear-response phenomenological theory. It is argued that the same type of behaviour is expected for any suspension of soft entities (capsules, red blood cells, etc.) that exhibit periodic motion under constant shear flow. We shall also discuss the reason why this type of behaviour could not have been captured by existing constitutive laws of complex fluids.

**Key words:** capsule/cell dynamics, suspensions

---

## 1. Introduction

Complex fluids are the rule in nature and in many industrial applications (Larson 1999). Examples are encountered in biology (blood, cartilage, etc.), the textiles, plastic and food industries, and many other situations. Most complex fluids (colloids,

<sup>†</sup> Email address for correspondence: [alexandr.farutin@ujf-grenoble.fr](mailto:alexandr.farutin@ujf-grenoble.fr)

emulsions, polymer solutions, blood, etc.) are made of rigid or soft particles that are suspended in a simple fluid. Understanding the rheology of complex fluids continues to pose a formidable challenge. The difficulty lies in the inherent coupling between the microscale (e.g. red blood cell (RBC) dynamics in the case of blood) and the macroscale (e.g. the scale of a vein). The micro–macro link implies that the laws describing complex fluids should carry information on the microscale dynamics.

Flow analysis (rheometry) of complex fluids determines several properties that are essential for building a progressive knowledge about the constitutive laws. The most commonly used experimental method to extract viscoelastic properties of complex fluids involves applying an oscillatory shear rate

$$\dot{\gamma} = \alpha \dot{\gamma}_0 \cos \omega t \quad (1.1)$$

(here  $\alpha \dot{\gamma}_0$  is a constant amplitude and  $\omega$  is the frequency) from which the complex viscosity  $\eta(\omega) = \eta'(\omega) + i\eta''(\omega)$  is extracted (Bird, Armstrong & Hassager 1987; Larson 1999). Its real part  $\eta'$  reflects the viscous character of the complex fluid (here  $G'' = \omega\eta'$  is called the loss modulus), while the imaginary part  $\eta''$  carries information on the elastic properties (here  $G' = \omega\eta''$  is called the storage modulus).

A more advanced, albeit less popular, way is to superimpose a constant shear rate on top of the oscillatory component

$$\dot{\gamma} = \dot{\gamma}_0(1 + \alpha \cos \omega t), \quad (1.2)$$

where  $\dot{\gamma}_0$  and  $\alpha$  are constant amplitudes. The difference can seem to be insignificant at the first sight and, indeed, conventional constitutive laws derived from macroscopic considerations show that the addition of a constant part to (1.2) leads only to quantitative change of the viscosity spectra. The same effect of superimposed steady shear rate was observed in experiments on polymer suspensions and melts (Booij 1966a,b; Tirtaatmadja, Tam & Jenkins 1997; Vlastos *et al.* 1997). A study of vesicle suspensions under combined oscillating and constant shear rates (Kantsler, Segre & Steinberg 2008) reported no noticeable effect of varying the constant part of the shear rate or the frequency of the oscillations. This was attributed to polydispersity of the suspension.

Recent experimental studies of rheology under constant shear flow of blood (Vitkova *et al.* 2008) and vesicle suspensions (Kantsler *et al.* 2008; Vitkova *et al.* 2008) reported that the intrinsic viscosity of these fluids critically depends on the viscosity of the solvent. This dependence is attributed to the difference in microscopic dynamics of individual particles: for high viscosity of the solvent, vesicles and RBCs experience so-called tank-treading (TT) motion, corresponding to a fixed orientation of the RBC or vesicle whereas the membrane moves like tank treads, while low viscosity of the solvent favours a tumbling (TB) motion. Remarkably, the stress produced by each particle oscillates dramatically over the TB cycle, as has been observed in analytical calculations (Danker & Misbah 2007; Vergeles 2008) and numerical simulations (Ghigliotti, Biben & Misbah 2010; Zhao & Shaqfeh 2011). An analogous effect has been observed in numerical simulations of dynamics of elastic capsules with compressible membranes (Clausen & Aidun 2010; Bagchi & Kalluri 2011). Thus, averaging over all particles in the suspension (or over time if the ergodicity assumption is valid) is necessary in order to obtain the effective viscosity. Another type of motion have been observed for vesicles. This motion couples oscillations of the orientation with strong ‘breathing’ deformations of the vesicle. This type of motion has been called vacillating-breathing (VB) (Misbah 2006; Danker *et al.* 2007; Farutin, Biben & Misbah 2010; Biben, Farutin & Misbah 2011), trembling (Kantsler & Steinberg 2006;

Lebedev, Turitsyn & Vergeles 2007; Vlahovska & Gracia 2007; Lebedev, Turitsyn & Vergeles 2008; Deschamps, Kantsler & Steinberg 2009) or swinging (Noguchi & Gompper 2007). A similar motion has been observed in simulations of extensible elastic capsules (Bagchi & Kalluri 2009; Yazdani, Kalluri & Bagchi 2011).

TT, TB and VB motions are excited by the presence of a constant shear rate. Therefore, applying just a pure oscillation (1.1) would make the vesicle undergo small oscillations without exhibiting the TT, TB or VB motion. Therefore, we expect the complex viscosity not to carry any information about these dynamics in this case. In contrast, imposing a flow such as that given by (1.2) would excite (thanks to the constant term) either TT, TB or VB (depending on structural and control parameters). Imposing the oscillating part on top of the constant shear rate will then allow us to distinguish one mode from another by studying the rheological response, as we show in this paper. In other words, imposing the shear rate (1.2) leads to completely different results: it allows us to probe the impact of microscopic dynamics (TT, TB and VB) on the viscoelastic properties of suspensions.

We shall see that application of (1.1) would give always the same type of complex viscosity in any region of parameter space. In contrast, application of (1.2) will provide a response (complex viscosity) that depends on the regions in parameter space. For example, we shall see that in the regions of TT the complex viscosity is entirely different from that in the TB or the VB regions. In other words, the viscosity carries information on the microscopic dynamics. With this respect the present theory is quite distinct from other theories using known constitutive laws for complex fluids. Usually, macroscopic constitutive laws average contributions over all possible orientations of particles. If we follow the same approach in our case in order to calculate the complex viscosity, our results would deliver a complex viscosity which has the same functional dependence irrespective of the region of parameter space.

Our analysis suggests that the classical constitutive laws (such as the Oldroyd B model) should be revisited by adopting the following approach: we should first determine the response of particles to oscillations in each orientation (as discussed in the present paper) and only then calculate the average. This method, albeit more difficult, has an important advantage: in general, the state of the suspension is not defined unambiguously by the stress. Thus the evolution of the stress, which is defined by the state of the suspension, does not have to depend solely on the stress and the imposed flow, but can have dependence on hidden variables lost in averaging when the stress of the suspension is calculated. We show below that, indeed, it is impossible to express the relaxation of the stress of a suspension of TB vesicles as a function of the imposed flow and the deviation of the macroscopic stress from a steady-state value. Instead, we shall take into account the state of each vesicle.

With this approach, we will explicitly show that the complex viscosity reveals new features. We shall see that the new qualitative features reported here cannot be reproduced by any reasonable macroscopic averaged constitutive law (e.g. the Oldroyd B model), in which averages are made before application of shear rate (1.2). This suggests that under addition of steady shear rate on top of oscillations, we should perform the average in the sense we suggest in order to extract much more insightful properties of  $\eta(\omega)$ .

### 1.1. The model

Our starting point is based on the microscopic constitutive law that has been recently derived for a dilute vesicle suspension where the vesicle is close to a spherical shape (Danker *et al.* 2007; Danker & Misbah 2007). We expect this analysis to

capture the essential features not only for vesicles, but also for capsules, and their biological counterparts, represented by RBCs. Dynamics of vesicles and capsules have been reviewed recently (Barthès-Biesel 2009; Vlahovska, Podgorski & Misbah 2009). A vesicle is a closed membrane separating two liquids. The membrane is made of a phospholipid bilayer, which can be regarded as an incompressible ideal two-dimensional fluid. The internal and external liquids can be taken as Newtonian with viscosities  $\eta_{int}$  and  $\eta_{ext}$ , respectively. The volume and the surface area  $A$  of the vesicle are conserved due to the incompressibility of the enclosed fluid and impermeability and incompressibility of the membrane. This means that vesicles, unlike droplets, can have non-spherical shapes even at the equilibrium. Weakly deflated vesicles assume an axisymmetric prolate shape.

The dynamics of a vesicle under steady shear flow (Danker *et al.* 2007) is governed by three dimensionless parameters: (i) the viscosity contrast

$$\lambda = \eta_{int}/\eta_{ext}; \tag{1.3}$$

(ii) the excess area

$$\Delta = A/r_0^2 - 4\pi, \tag{1.4}$$

measuring the deflation of the vesicle; and (iii) the capillary number

$$C_a = \eta_{ext}\dot{\gamma}_0 r_0^3/\kappa, \tag{1.5}$$

which is the shear rate rescaled by characteristic shape relaxation time. Here  $r_0$  is the radius of a sphere containing the same volume as the vesicle and  $\kappa$  is the bending rigidity coefficient of the membrane. We chose our units in such a way that  $\kappa = 1$ ,  $r_0 = 1$  and  $\eta_{ext} = 1$ . When the viscosity contrast is low enough, the TT motion prevails under shear flow, i.e. the shape and orientation of the vesicle relax to a certain steady state, which depends on the parameters  $\lambda$ ,  $\Delta$  and  $C_a$ . If the viscosity contrast is high, the vesicle dynamics under shear flow relaxes to a periodic TB motion, in which the vesicle experiences almost solid-like rotation in the shear plane. For later purposes, we found it worthwhile to recall the regions of stability of each motion in figure 1. The transition from TT to TB region occurs directly via a saddle-node bifurcation for small  $C_a$ . For higher  $C_a$ , there is a band between TT and TB regions where vesicle dynamics relaxes to intermediate VB motion, during which the vesicle lies in the shear plane and its longest axis oscillates periodically about the flow direction, while the shape changes accordingly. The transition from TT to VB region occurs via a Hopf bifurcation (Danker *et al.* 2007; Lebedev *et al.* 2007, 2008).

Vesicles are characterized by their conformation (shape and orientation), which is, to leading order, an ellipsoid. The deviation of the shape from a sphere can thus be parametrized by a quadratic form  $r_i r_j F_{ij}(t)$ , where  $r_i$  is the  $i$ th Cartesian component of the position vector  $\mathbf{r}$ . The conservation of the enclosed volume and excess area  $\Delta$  impose (Danker *et al.* 2007) two relations among the components of  $\mathbf{F}$ :

$$\text{Tr } \mathbf{F} = 0, \quad \text{Tr } \mathbf{F}^2 = \frac{5}{48\pi}, \tag{1.6}$$

so that we are left with four independent amplitudes  $F_{ij}$ . The question amounts to determining the evolution equation for  $F_{ij}(t)$ . This can be achieved by solving

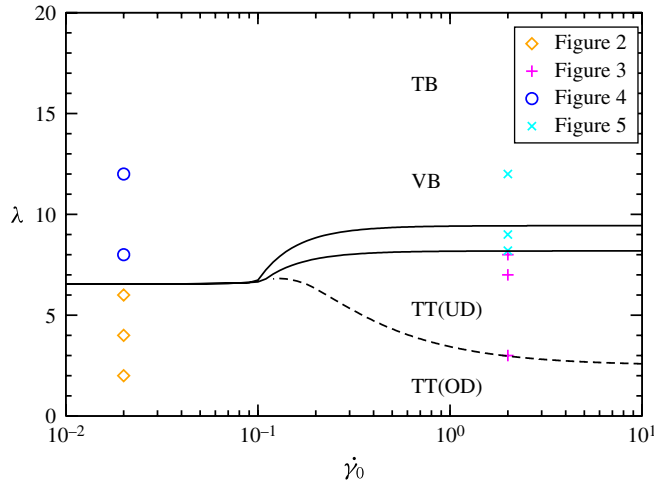


FIGURE 1. (Colour online available at [journals.cambridge.org/flm](http://journals.cambridge.org/flm)) The phase diagram distinguishing regions of TT, VB and TB motions for  $\Delta = 0.25$ . The marked points denote the parameters for which the complex viscosity is studied in the present paper. They are grouped according to the figure on which the spectra are presented. The dashed line separates the regions of TT motion with underdamped (UD) and overdamped (OD) relaxation.

the Stokes equations with boundary conditions at the membrane, which leads to a differential equation for  $F_{ij}(t)$  (Danker *et al.* 2007)

$$\frac{\partial F_{ij}}{\partial t} = f_{ij}[F_{i'j'}, \dot{\gamma}(t)] \tag{1.7}$$

where  $f_{ij}$  is a nonlinear function determined in Danker *et al.* (2007).

Let the imposed flow be  $\mathbf{V}(x, y, z) = (\dot{\gamma}y, 0, 0)$ . Then the effective viscosity is defined as

$$\eta = \Sigma_{xy}/\dot{\gamma}, \tag{1.8}$$

where the stress tensor of the composite fluid  $\Sigma$  is a function of the vesicle conformation. It can be written as

$$\Sigma_{ij} = \eta_{ext}(\partial_i V_j + \partial_j V_i) + \phi \langle \sigma_{ij} \rangle, \tag{1.9}$$

where  $\eta_{ext}(\partial_i V_j + \partial_j V_i)$  is the stress of the pure solvent, while  $\phi \langle \sigma_{ij} \rangle$  accounts for the vesicle contribution ( $\phi$  is the volume fraction of the vesicles; we consider the dilute regime) and  $\langle \rangle$  refers to averaging over a large number of independent vesicles. The stress produced by each vesicle is a function of its conformation and the imposed shear rate

$$\sigma_{ij}(t) = s_{ij}[F_{i'j'}(t), \dot{\gamma}(t)], \tag{1.10}$$

i.e. the effective viscosity of a suspension of VB/TB vesicles appears to be independent of time only as a consequence of averaging over a large number of particles whose phases of VB/TB motion are randomly distributed. The functions  $f_{ij}$  and  $s_{ij}$  are nonlinear and quite lengthy but their exact expressions are not important for our purposes. They are listed in the appendices A and B for completeness.

Assuming that amplitude of the oscillations (1.2)  $\alpha\dot{\gamma}_0$  is small, we can expect that the stress of the suspension can be expanded in powers of  $\alpha$  :

$$\Sigma_{xy}(t) = \Sigma_{xy}^{(0)} + \alpha \Sigma_{xy}^{(1)}(t) + O(\alpha^2), \tag{1.11}$$

where

$$\Sigma_{xy}^{(0)} = \eta_{ext} \dot{\gamma}_0 + \phi \langle \sigma_{xy}^{(0)} \rangle, \tag{1.12}$$

$$\Sigma_{xy}^{(1)}(t) = \eta_{ext} \dot{\gamma}_0 \cos(\omega t) + \phi \langle \sigma_{xy}^{(1)}(t) \rangle. \tag{1.13}$$

Note that, as discussed above, we shall first expand  $\sigma$  in powers of  $\alpha$  and then take the averaging in order to calculate  $\langle \sigma_{xy}^{(1)}(t) \rangle$ .

We shall see in the appendix C when this expansion is appropriate. Substituting (1.2) and (1.11) into (1.8), we get

$$\begin{aligned} \eta(t) &= \frac{\Sigma_{xy}^{(0)}}{\dot{\gamma}_0} + \alpha \left( \frac{\Sigma_{xy}^{(1)}(t)}{\dot{\gamma}_0} - \frac{\Sigma_{xy}^{(0)}}{\dot{\gamma}_0} \cos(\omega t) \right) + O(\alpha^2) \\ &= \eta^{(0)} + \alpha \left( \frac{\Sigma_{xy}^{(1)}(t)}{\dot{\gamma}_0} - \eta^{(0)} \cos(\omega t) \right) + O(\alpha^2), \end{aligned} \tag{1.14}$$

where  $\eta^{(0)}$  is the effective viscosity of the suspension under steady shear flow, which has been already analysed by Danker *et al.* (2007), Danker & Misbah (2007) and Vergeles (2008). We are interested here in the part of the viscosity that is linear in the amplitude of the oscillations (i.e. is proportional to  $\alpha$ ) and has the same frequency  $\omega$ . Extracting the Fourier component of  $\eta(t)$  corresponding to the frequency  $\omega$ , we get

$$\eta'(\omega) = \alpha \phi \left( \frac{\langle \sigma_{xy}^{(1)'}(\omega) \rangle}{\dot{\gamma}_0} - \eta_0 \right), \quad \eta''(\omega) = \alpha \phi \frac{\langle \sigma_{xy}^{(1)''}(\omega) \rangle}{\dot{\gamma}_0}, \tag{1.15}$$

where  $\eta_0 = \langle \sigma_{xy}^{(0)} \rangle / \dot{\gamma}_0$  is the intrinsic viscosity of the suspension under steady shear flow. The value of  $\sigma_{xy}^{(1)'}(\omega) = \sigma_{xy}^{(1)'}(\omega) + i \sigma_{xy}^{(1)''}(\omega)$ , the Fourier component of the  $\alpha$  term in the expansion of  $\sigma_{xy}(t)$ , is obtained by numerical solution of (1.7) and (1.10). For simplicity, below we shall use intrinsic complex viscosity defined by

$$\eta_1(\omega) = \eta(\omega) / (\alpha \phi). \tag{1.16}$$

## 2. Analysis of rheology in the TT phase

The results are presented in figures 2 and 3 (all calculations were performed for  $\Delta = 0.25$ ). We have investigated  $\eta_1(\omega)$  both for a small shear rate,  $\dot{\gamma}_0 = 0.02$ , and a larger one,  $\dot{\gamma}_0 = 2$ . Comparison of figure 2 (low  $\dot{\gamma}_0$ ) and figure 3 (higher  $\dot{\gamma}_0$ ) reveals an important qualitative difference: in the TT regime the vesicle behaviour is qualitatively the same for both shear rates (from the conformational point of view) while the complex viscosities are entirely different. Rheology thus highlights subtle hidden features that cannot be deduced by simply visualizing the vesicle conformation.

The understanding of this behaviour is related to the fact that in the TT regime the vesicle, when driven away from its steady regime, relaxes to its fixed point (TT regime) either in a monotonous way (OD, overdamped relaxation) or by exhibiting damped oscillations (UD, underdamped relaxation). The dependence of the relaxation type on the vesicle parameters has been found by Lebedev *et al.* (2007, 2008). Here we confirm these findings using our model: oscillations take place at high enough

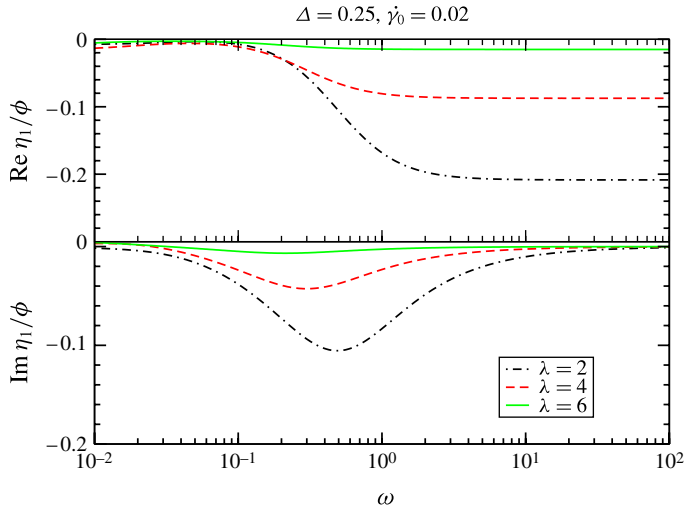


FIGURE 2. (Colour online) Complex viscosity in the TT phase for lower  $\dot{\gamma}_0$ .

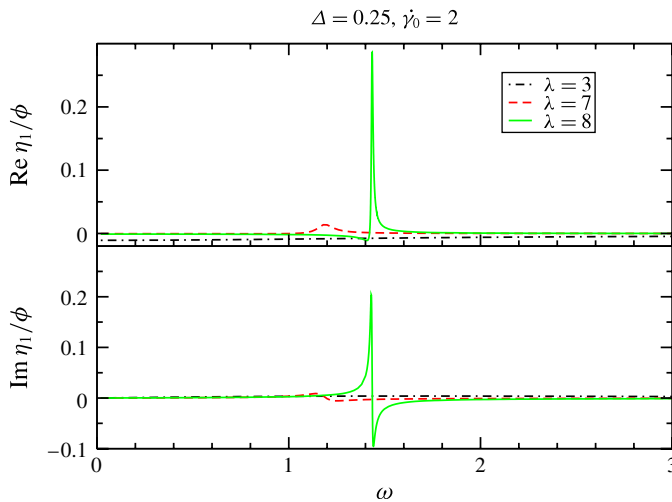


FIGURE 3. (Colour online) Complex viscosity in the TT phase for higher  $\dot{\gamma}_0$ .

shear rates and viscosity contrast. The phase diagram in figure 1 shows the region of parameter space where damped oscillations occur. As it happens for macroscopic constitutive laws, the complex viscosity  $\eta_1(\omega)$  of TT vesicles is defined by the way vesicle motion relaxes to the steady-state behaviour. The microscopic law, however, allows the characteristic relaxation times to be related to the properties of vesicle dynamics. As seen above, vesicles relax to TT motion monotonously in weak flows and after a transient of damped oscillations for strong flows and high enough viscosity contrasts. When the frequency of the imposed oscillations is close to the frequency of the damped oscillations, a resonance occurs. The closer the TT/VB phase border is (by increasing  $\lambda$ ), the slower the decay of the damped oscillations is and the more pronounced the resonance peaks are. In region where the TT regime is OD, no

resonance can take place. This explains qualitatively the major difference between the behaviour of  $\eta_1(\omega)$  at low and high shear rate.

Actually, it is possible to gain more insight with phenomenological approach: the exact expression for  $\eta_1(\omega)$  in the TT phase can be found using linear response approximation (i.e. by assuming the amplitude  $\alpha$  of the applied oscillating shear rate to be small enough). For ease of presentation, we use complex shear rate  $\dot{\gamma}(t) = \dot{\gamma}_0(1 + \alpha e^{i\omega t})$ . In order to obtain the various quantities (e.g. the viscosity) corresponding to the real shear rate (1.2) we simply need to take the real part of the solutions thanks to the linear response approximation. We write

$$F_{ij}(t) = F_{ij}^{(0)}(t) + \alpha F_{ij}^{(1)}(t), \tag{2.1}$$

where  $F_{ij}^{(0)}(t)$  is the solution for the constant shear rate  $\dot{\gamma}_0$ . Substituting (2.1) into (1.7) and (1.10) and expanding in  $\alpha$ , we get

$$\dot{F}_{ij}^{(1)}(t) = \frac{\partial f_{ij}}{\partial F_{i'j'}}(t) F_{i'j'}^{(1)}(t) + \dot{\gamma}_0 \frac{\partial f_{ij}}{\partial \dot{\gamma}}(t) e^{i\omega t} + O(\alpha), \tag{2.2}$$

$$\sigma_{ij}^{(1)}(t) = \frac{\partial s_{ij}}{\partial F_{i'j'}}(t) F_{i'j'}^{(1)}(t) + \dot{\gamma}_0 \frac{\partial s_{ij}}{\partial \dot{\gamma}}(t) e^{i\omega t} + O(\alpha). \tag{2.3}$$

The partial derivatives in (2.2) and (2.3) should be evaluated using the solution of (1.7) for  $\dot{\gamma}(t) = \dot{\gamma}_0$ . This means that they are independent of time for TT motion (since the vesicle conformation function,  $F_{ij}^{(0)}(t)$ , which enters the above derivative, is independent of time). TT vesicles possess mirror symmetry  $z \rightarrow -z$  about the shear plane, implying that  $F_{xz} = F_{yz} = 0$ . The oscillations of the shear rate do not break this symmetry and thus cannot excite  $F_{xz}$  and  $F_{yz}$ . The constraints (1.6) leave us with only two possible linearly independent deviations of  $F_{ij}$ , denoted as  $\varphi_{ij}^1$  and  $\varphi_{ij}^2$ . Now  $F_{ij}^{(1)}$ ,  $\partial f_{ij} / \partial F_{i'j'} \varphi_{i'j'}^b$  and  $\partial f_{ij} / \partial \dot{\gamma}$  can be represented as linear combinations of  $\varphi_{ij}^a$ , ( $a, b \in \{1, 2\}$ ):

$$F_{ij}^{(1)}(t) = \xi_a \varphi_{ij}^a, \quad \frac{\partial f_{ij}}{\partial F_{i'j'}} \varphi_{i'j'}^b = J_{ab} \varphi_{ij}^a, \quad \frac{\partial f_{ij}}{\partial \dot{\gamma}} = G_a \varphi_{ij}^a. \tag{2.4}$$

Using this notation and the fact that the matrices  $\varphi_{ij}^a$  form a basis in the subspace of possible deviations, we can rewrite the (2.2) in a simpler way:

$$\dot{\xi}_a(t) = J_{ab} \xi_b(t) + \dot{\gamma}_0 G_a e^{i\omega t}. \tag{2.5}$$

Substituting  $\xi_a(t) = \xi_a(\omega) e^{i\omega t}$ , we get

$$\xi(\omega) = \dot{\gamma}_0 [i\omega I - \mathbf{J}]^{-1} \cdot \mathbf{G}, \tag{2.6}$$

where  $I$  is the identity matrix. Denoting

$$H_a = \frac{\partial s_{xy}}{\partial F_{ij}} \varphi_{ij}^a, \tag{2.7}$$

we can write

$$\sigma_{xy}^{(1)}(t) = \dot{\gamma}_0 \left[ \mathbf{H} \cdot (i\omega I - \mathbf{J})^{-1} \cdot \mathbf{G} + \frac{\partial s_{xy}}{\partial \dot{\gamma}} \right] e^{i\omega t}. \tag{2.8}$$

The Jacobian matrix has in principle two distinct eigenvalues  $\nu_1$  and  $\nu_2$ . Diagonalizing  $\mathbf{J}$  and using primes to refer to the components of vectors in the basis in which  $\mathbf{J}$  is



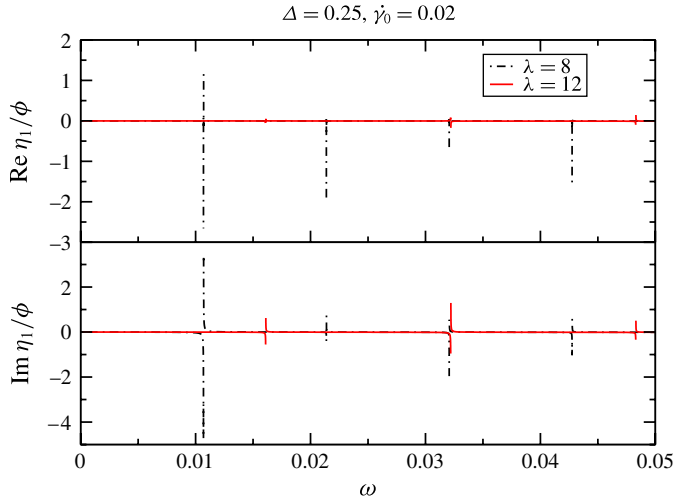


FIGURE 4. (Colour online) Complex viscosity in TB phase for low enough  $\gamma_0$ .

diagonal, we get

$$\eta_1 = \eta_{1\infty} + \sum_{j=1}^2 \frac{X_j}{i\omega - v_j}, \tag{2.9}$$

where  $X_a = G'_a H'_a$  (no summation implied) and  $\eta_{1\infty} = \partial s_{xy} / \partial \dot{\gamma} - \eta_0$  are independent of frequency. The overdamping of the relaxation occurs when both eigenvalues are real, while the relaxation is UD for complex eigenvalues. In the UD region, the non-zero imaginary part of  $v_i$  implies, in light of (2.9), a resonance in the spectrum. Note that the extreme value attained by  $\eta_1$  is located close to  $\omega = |\text{Im}(v_i)|$ . Finally,  $\eta_1(\omega)$  diverges for  $\omega = |\text{Im}(v_i)|$  if  $\text{Re}(v_i) \rightarrow 0$ . When this condition is met, this means that the TT regime is at the border of the loss of its stability against the VB mode. In other words, the analysis of the effective viscosity can be used as a ‘blind’ probe to detect the bifurcation from the TT into the VB regime. We have found that one of the eigenvalues becomes equal to zero at the border of transition from TT to TB motion (in agreement with Lebedev *et al.* (2007, 2008)), but  $\eta_1(\omega)$  remains finite for any  $\omega$ .

Finally, we have checked that by solving the full nonlinear (1.7) we find a good agreement with our linear response theory.

### 3. Analysis of rheology in the VB/TB phases

The results for VB and TB phases are presented in figures 4 and 5. Motion of VB/TB vesicles is periodic and thus can be represented as a Fourier series. Each harmonic in this series can be excited by the imposed oscillations. This leads to spectra with resonances not only at the VB/TB frequency  $\Omega$  but also at its multiples.

The (2.2) is not as easy to solve for VB/TB vesicles as in case of TT motion. Nevertheless, an expression for  $\eta_1(\omega)$  can be derived by exploiting the periodicity of VB/TB motions.

Let us first consider a homogeneous equation

$$\dot{F}_{i,j}^{(1)}(t) = \frac{\partial f_{i,j}}{\partial F_{i',j'}}(t) F_{i',j'}^{(1)}(t). \tag{3.1}$$

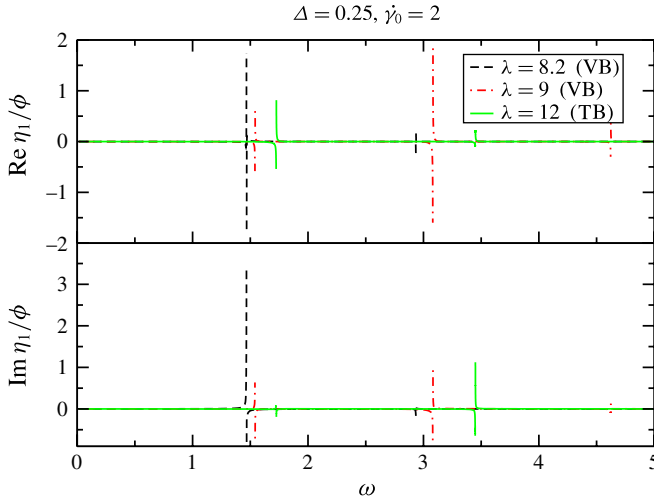


FIGURE 5. (Colour online) Complex viscosity in TB/VB phases for higher  $\dot{\gamma}_0$ .

The partial derivatives  $\partial f_{i,j} / \partial F_{i',j'}$  are calculated at the limit cycle of the VB/TB motion and are thus periodic. Using the Floquet’s theorem, we express the solutions of the (3.1) as

$$F_{i,j}^{(1)}(t) = \xi_a e^{iR_{ab}t} \varphi_{i,j}^b(t), \tag{3.2}$$

where  $\xi_a$  are constants defining the particular solution,  $R_{ab}$  is a constant matrix and  $\varphi_{i,j}^b(t)$  is some function having the same period as the VB/TB motion,

$$\varphi_{i,j}^b(t) = \varphi_{i,j}^b(t + T), \quad T = 2\pi/\Omega. \tag{3.3}$$

The indices  $a, b$  run from 1 to 6 for a general problem, but the basic solutions  $e^{R_{ab}t} \varphi_{i,j}^b(t)$  can be chosen in such a way that exactly two of them,  $e^{R_{ab}t} \varphi_{i,j}^b(t)$  with  $a$  and  $b$  running from 1 to 2, will satisfy the constraints

$$F_{i,i}^{(1)}(t) = 0, \quad F_{i,j}^{(1)}(t)F_{i,j}^{(0)}(t) = 0, \quad F_{xz}^{(1)}(t) = 0, \quad F_{yz}^{(1)}(t) = 0, \tag{3.4}$$

which represent the fact that the perturbed solution describes a vesicle of the same volume, surface area and  $z \rightarrow -z$  symmetry as the unperturbed solution does. Later we will only consider these two deviations because the others cannot be excited by the oscillations of the shear rate.

The relaxation of the solutions (3.2) to zero is defined by the eigenvalues of the matrix  $R_{ab}$ . It is known (and can be checked by a straightforward substitution) that the time derivative of the undisturbed limit-cycle solution,  $\dot{F}_{i,j}^{(0)}(t)$ , satisfies the (3.1). Since this function has the same periodicity in time as the limit-cycle solution  $F_{i,j}^{(0)}(t)$  itself, we conclude that this solution is an eigenvector of  $e^{TR_{ab}}$  and the corresponding eigenvalue is equal to 1. The second eigenvalue of  $e^{TR_{ab}}$  must be real and comprised between 0 and 1. The upper boundary comes from the fact that the limit cycle is stable. The lower one comes from the fact that  $F_{i,j}^{(1)}(t)$  lie in the tangent bundle of an ellipsoid defined by the constraints (1.6) and  $F_{xz} = F_{yz} = 0$ . Ellipsoid is an orientable surface and, consequently,  $\det e^{TR_{ab}} > 0$ . The solution (3.2) can thus be rewritten as

$$F_{i,j}^{(1)}(t) = \xi_1 \dot{F}_{i,j}^{(0)}(t) + \xi_2 e^{\nu t} \varphi_{i,j}(t), \tag{3.5}$$

where  $e^{T\nu}$  and  $\varphi_{i,j}(t)$  are the second eigenvalue and the second eigenvector of  $e^{TRab}$ . The Floquet exponent  $\nu$  is defined modulo  $i\Omega$  and, for convenience, we choose it to be real. In this case, the matrix  $\varphi_{i,j}(t)$  is also real. Since  $e^{T\nu} < 1$ , we conclude that  $\nu$  is negative.

Now we can use the classical method of variation of the coefficients  $\xi_a$  in order to solve the inhomogeneous system (2.2). Owing to the symmetry of the flow and volume and surface area conservation, the values of  $\partial f_{i,j} / \partial \dot{\gamma}$  satisfy the constraints equivalent to (3.4):

$$\frac{\partial f_{i,i}}{\partial \dot{\gamma}}(t) = 0, \quad \frac{\partial f_{i,j}}{\partial \dot{\gamma}}(t) F_{i,j}^{(0)}(t) = 0, \quad \frac{\partial f_{xz}}{\partial \dot{\gamma}}(t) = 0, \quad \frac{\partial f_{yz}}{\partial \dot{\gamma}}(t) = 0. \tag{3.6}$$

Because  $\dot{F}_{i,j}^{(0)}(t)$  and  $\varphi_{i,j}(t)$  make a basis in the space of matrices satisfying the constraints (3.4) at each moment of time  $t$ , we can write

$$\frac{\partial f_{i,j}}{\partial \dot{\gamma}}(t) = G_1(t) \dot{F}_{i,j}^{(0)}(t) + G_2(t) \varphi_{i,j}(t), \tag{3.7}$$

where  $G_a(t)$  are certain periodic functions. Now we consider  $\xi_a$  to be functions of time and plug (3.5) into (2.2), after using the fact that  $\dot{F}_{i,j}^{(0)}(t)$  and  $e^{\nu t} \varphi_{i,j}(t)$  are solutions of the homogeneous system (3.1) to cancel some terms, we get

$$[\dot{\xi}_1(t) - \dot{\gamma}_0 e^{i\omega t} G_1(t)] \dot{F}_{i,j}^{(0)}(t) + [\dot{\xi}_2(t) e^{\nu t} - \dot{\gamma}_0 e^{i\omega t} G_2(t)] \varphi_{i,j}(t) = 0. \tag{3.8}$$

Because  $\dot{F}_{i,j}^{(0)}(t)$  and  $\varphi_{i,j}(t)$  are linearly independent (as matrices) at each moment of time  $t$ , we find that

$$\xi_1(t) = \xi_1^{(0)} + \dot{\gamma}_0 \int_0^t G_1(\tau) e^{i\omega\tau} d\tau, \quad \xi_2(t) = \xi_2^{(0)} + \dot{\gamma}_0 \int_0^t G_2(\tau) e^{(i\omega - \nu)\tau} d\tau. \tag{3.9}$$

The functions  $G_a(t)$ , being periodic in time, can be expanded into Fourier series:

$$G_a(t) = \sum_{k=-\infty}^{\infty} g_{a,k} e^{ik\Omega t}. \tag{3.10}$$

Substituting (3.10) into (3.9), we get

$$\left. \begin{aligned} \xi_1(t) &= \xi_1^{(0)} + \dot{\gamma}_0 e^{i\omega t} \sum_{k=-\infty}^{\infty} \frac{g_{1,k} e^{ik\Omega t}}{i(\omega + k\Omega)}, \\ \xi_2(t) &= \xi_2^{(0)} + \dot{\gamma}_0 e^{(i\omega - \nu)t} \sum_{k=-\infty}^{\infty} \frac{g_{2,k} e^{ik\Omega t}}{i(\omega + k\Omega) - \nu}. \end{aligned} \right\} \tag{3.11}$$

Now we substitute (3.11) into (3.5) and the result into (2.3). We get

$$\begin{aligned} \sigma_{xy}^{(1)}(t) &= \frac{\partial s_{xy}}{\partial F_{i,j}}(t) \left[ \dot{F}_{i,j}^{(0)}(t) \left( \xi_1^{(0)} + \dot{\gamma}_0 e^{i\omega t} \sum_{k=-\infty}^{\infty} \frac{g_{1,k} e^{ik\Omega t}}{i(\omega + k\Omega)} \right) \right. \\ &\quad \left. + \varphi_{i,j}(t) \left( \xi_2^{(0)} e^{\nu t} + \dot{\gamma}_0 e^{i\omega t} \sum_{k=-\infty}^{\infty} \frac{g_{2,k} e^{ik\Omega t}}{i(\omega + k\Omega) - \nu} \right) \right] + \dot{\gamma}_0 \frac{\partial s_{xy}}{\partial \dot{\gamma}}(t) e^{i\omega t}. \end{aligned} \tag{3.12}$$

To simplify this expression, we calculate the time derivative of the stress in undisturbed VB/TB motion

$$\dot{s}_{xy}^{(0)}(t) = \frac{\partial s_{xy}}{\partial F_{ij}}(t) \dot{F}_{ij}^{(0)}(t), \tag{3.13}$$

and note that  $\xi_2^{(0)} e^{\nu t}$  can be omitted because  $e^{\nu t}$  decays with time. The resulting expression is

$$\begin{aligned} \sigma_{xy}^{(1)}(t) = & \xi_1^{(0)} \dot{s}_{xy}^{(0)}(t) + \dot{\gamma}_0 e^{i\omega t} \left[ \sum_{k=-\infty}^{\infty} \frac{\dot{s}_{xy}^{(0)}(t) g_{1,k} e^{ik\Omega t}}{i(\omega + k\Omega)} \right. \\ & \left. + \sum_{k=-\infty}^{\infty} \frac{H(t) g_{2,k} e^{ik\Omega t}}{i(\omega + k\Omega) - \nu} + \frac{\partial s_{xy}}{\partial \dot{\gamma}}(t) \right], \end{aligned} \tag{3.14}$$

where  $H(t) = \varphi_{ij}(t) \partial s_{xy} / \partial F_{ij}(t)$ . As can be seen from (3.14), the suspension of VB/TB vesicles shows linear response not only at the input frequency  $\omega$ , but also at integer multiples of the VB/TB frequency  $\Omega$  (coming from the first part of (3.14)) and frequencies of the form  $\omega + k\Omega$  with integer  $k$  (coming from the second part of (3.14)). Nevertheless, we only calculate the response at the frequency  $\omega$ , for which we assume that  $\omega/\Omega$  is not an integer. In practice, the closer  $\omega$  is to a multiple of  $\Omega$ , the longer is the period of time over which  $\sigma_{xy}^{(1)}(t)$  needs to be measured in order to extract the response at the frequency  $\omega$ . Using the periodicity of  $\dot{s}_{xy}^{(0)}(t)$  and  $H(t)$ , we set

$$\dot{s}_{xy}^{(0)}(t) = \sum_{k=-\infty}^{\infty} h_{1,k} e^{ik\Omega t}, \quad H(t) = \sum_{k=-\infty}^{\infty} h_{2,k} e^{ik\Omega t}. \tag{3.15}$$

Substituting these definitions into (3.14) and extracting the Fourier component at the frequency  $\omega$ , we get

$$\eta_1 = \eta_{1\infty} + \sum_{k=-\infty}^{\infty} \frac{X_{1,k}}{i(\omega + k\Omega)} + \sum_{k=-\infty}^{\infty} \frac{X_{2,k}}{i(\omega + k\Omega) - \nu}, \tag{3.16}$$

where  $X_{a,k} = h_{a,-k} g_{a,k}$  (no summation implied) and

$$\eta_{1\infty} = \frac{1}{T} \int_0^T \frac{\partial s_{xy}}{\partial \dot{\gamma}}(\tau) d\tau - \eta_0. \tag{3.17}$$

The expression (3.16) diverges as  $\omega$  tends to an integer multiple of  $\Omega$ . This effect is a consequence of the linear response approximation: the deviations of  $F_{ij}$ , that diverge, correspond to the motion on the limit cycle. In other words, the application of the oscillating shear rate makes the VB/TB motion irregular, such that the phase of VB/TB oscillates in time. Because the effective viscosity produced by VB/TB vesicles is finite,  $\eta_1(\omega)$  does not diverge even for large oscillations of the phase of VB/TB motion. A more detailed discussion of this fact can be found in the appendix C.

The following method is used to obtain the spectra numerically for VB/TB phases: the exciting frequencies are chosen to be commensurate with the frequency of VB/TB motion. Then the period of time, over which the viscosity has to be measured, is the least positive common multiple of  $\Omega$  and  $\omega$ . We chose the step of  $\omega$  to be  $\Omega/2000$ , which requires to integrate the response in the viscosity over 2000 periods of VB/TB motion in order to extract the corresponding Fourier component of the stress. On experiment, such long integration is meaningless, since the periodicity of

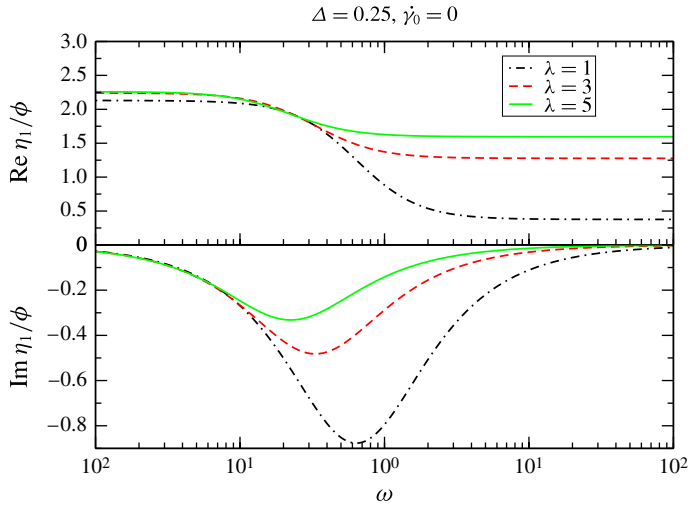


FIGURE 6. (Colour online) Complex viscosity for vesicles perpendicular to the shear plane when  $\dot{\gamma}_0 = \alpha \dot{\gamma}_0 \cos(\omega t)$ .

VB/TB motion will be compromised by many factors, such as thermal noise and hydrodynamic interactions. Reduction of the integration time leads to the appearance of noise in the vicinity of the resonance frequencies.

#### 4. Discussion

Our results have shown that the application of an oscillating part  $\alpha \dot{\gamma}_0 \cos \omega t$  (as is done in several classical analyses of complex fluids) plus a constant shear rate reveals several resonances in the complex viscosity. This expresses the fact that intrinsic oscillating modes are excited whenever the oscillating frequency is equal to an integer value of the intrinsic frequency of the TB or VB modes. In addition to the importance for rheology itself, this idea can be used as a probe to determine the period of oscillations of isolated entities. This will be valid as long as one considers dilute enough suspensions for the pair hydrodynamic interaction to be negligible. In the semi-dilute regime one expects interaction to shift and broaden resonance peaks.

The main message is the importance of the superposition of a constant shear flow to the pure oscillation. For that purpose, consider the case where only a sinusoidal shear rate  $\dot{\gamma} = \alpha \dot{\gamma}_0 \cos(\omega t)$  is retained (this form of shear rate is the commonly used one in analysis of viscoelastic effects of many complex fluids) and analyse the resulting viscosity from our constitutive equations. The results are shown in figure 6. The results of that figure differ markedly from those in figures 3–5. Imposing a standard excitation,  $\dot{\gamma} = \alpha \dot{\gamma}_0 \cos(\omega t)$ , induces no preferable orientation of the vesicles regardless of the value of the control parameters in the phase diagram of figure 1. Consequently, the vesicles oscillate about their initial positions with the proviso that  $\alpha \dot{\gamma}_0$  be small enough (in addition, the amplitude of these oscillations is small if  $\alpha \dot{\gamma}_0 \ll \omega$ ). The response of the suspension is averaged over all possible orientations of the vesicles in this case.

The results for VB/TB motions can not be explained within the framework of conventional phenomenological constitutive laws: such laws predict steady-state stress under a constant shear rate, which is not the case for VB/TB vesicles. The response of such systems to an application of small oscillation is defined by their relaxation

towards the steady state. We would like to illustrate our remark on a popular Oldroyd B model (Bird *et al.* 1987; Larson 1999). This model is widely used in many contexts, and especially for dilute polymer solutions. The constitutive law in the Oldroyd model is given by

$$\tau[\dot{\sigma} - \sigma \cdot \nabla \otimes \mathbf{V} - (\nabla \otimes \mathbf{V})^T \cdot \sigma] + \sigma = \eta_0(\nabla \otimes \mathbf{V} + \nabla \otimes \mathbf{V}^T), \tag{4.1}$$

where the dot stands for material derivative,  $\tau$  is a characteristic relaxation time (the relaxation of the Hookean spring of the dumbbell model) of the system,  $\sigma$  is the intrinsic stress produced by the polymers and  $\eta_0$  is a characteristic viscosity associated with the polymers. For the imposed flow  $\mathbf{V}(x, y, z) = (\dot{\gamma}y, 0, 0)$ , we get

$$\tau \dot{\sigma}_{xy} - \dot{\gamma} \tau \sigma_{yy} + \sigma_{xy} = \eta_0 \dot{\gamma} \tag{4.2}$$

$$\tau \dot{\sigma}_{yy} + \sigma_{yy} = 0. \tag{4.3}$$

Equation (4.3) shows that  $\sigma_{yy}$  relaxes to 0 regardless of the initial value. This allows us to exclude it from (4.2):

$$\tau \dot{\sigma}_{xy} + \sigma_{xy} = \eta_0 \dot{\gamma}. \tag{4.4}$$

We see that (4.4) is linear despite the nonlinearity of the initial equation (4.1). This is a consequence of particulate configuration of the flow, e.g. the nonlinear terms survive if the oscillations are applied perpendicularly to the steady part. Under steady shear flow, the viscosity is  $\eta_0$ . If only oscillating shear rate  $\dot{\gamma} = \alpha \dot{\gamma}_0 e^{i\omega t}$  is applied, the stress has only oscillating part as well:

$$\sigma_{xy}(t) = \frac{\alpha \dot{\gamma}_0 \eta_0}{1 + i\omega\tau} e^{i\omega t}. \tag{4.5}$$

If we divide the stress by the shear rate, we get a quantity that is independent of time:

$$\eta(\omega) = \frac{\sigma_{xy}(t)}{\dot{\gamma}(t)} = \frac{\eta_0}{1 + i\omega\tau}. \tag{4.6}$$

When steady and oscillating shear flows are combined  $\dot{\gamma} = \dot{\gamma}_0 (1 + \alpha e^{i\omega t})$ , the oscillating part of the stress is the same as under the imposed flow  $\dot{\gamma} = \alpha \dot{\gamma}_0 e^{i\omega t}$  because of the linearity of (4.4):  $\sigma_{xy}(t) = \sigma_{xy}^{(0)} + \alpha \sigma_{xy}^{(1)}(t)$ , where

$$\sigma_{xy}^{(0)} = \dot{\gamma}_0 \eta_0, \quad \sigma_{xy}^{(1)}(t) = \frac{\dot{\gamma}_0 \eta_0}{1 + i\omega\tau} e^{i\omega t}. \tag{4.7}$$

That is, the oscillating part of the stress tensor is the same in both cases (compare (4.5) and (4.7)). Since the rheometric devices deliver the torque (proportional to the stress), one would *a priori* see no difference between the two situations. However, we can still see theoretically some differences on the viscosity as shown below.

Calculating the complex viscosity, we get

$$\eta(\omega) = \frac{\sigma_{xy}(t)}{\dot{\gamma}(t)} = \eta_0 \left[ 1 + \alpha \frac{e^{i\omega t}}{(1 + i\omega\tau)} \right] (1 + \alpha e^{i\omega t})^{-1} = \eta_0 - \alpha \frac{i\omega\tau \eta_0}{1 + i\omega\tau} e^{i\omega t}. \tag{4.8}$$

From which we get (cf. (1.16)),

$$\eta_1(\omega) = -\frac{i\omega\tau \eta_0}{1 + i\omega\tau}. \tag{4.9}$$

Actually, the degeneracy of the results in stresses (equations (4.5) and (4.7)) is a consequence of the simplicity of the Oldroyd B model. The situation is different if we

take another constitutive equation, e.g. if we replace the upper convective derivative in (4.1) with the Jaumann derivative, the half-sum of the upper and the lower derivatives (see appendix A):

$$\tau \frac{\mathcal{D}\sigma}{\mathcal{D}t} + \sigma = \eta_0(\nabla \otimes \mathbf{V} + \nabla \otimes \mathbf{V}^T). \quad (4.10)$$

Equation (4.10) can be regarded as a very simple constitutive equation for a dilute emulsion (cf. Cox 1969; Frankel & Acrivos 1970). The intrinsic time  $\tau$  defines the characteristic time of relaxation of droplet shape to a sphere when no flow is applied.

Writing in coordinates, we get

$$\tau(\dot{\sigma}_{xx} - \dot{\gamma}\sigma_{xy}) + \sigma_{xx} = 0, \quad (4.11)$$

$$\tau \left[ \dot{\sigma}_{xy} + \frac{\dot{\gamma}}{2}(\sigma_{xx} - \sigma_{yy}) \right] + \sigma_{xy} = \eta_0\dot{\gamma}, \quad (4.12)$$

$$\tau(\dot{\sigma}_{yy} + \dot{\gamma}\sigma_{xy}) + \sigma_{yy} = 0. \quad (4.13)$$

Under constant shear rate  $\dot{\gamma} = \dot{\gamma}_0$ , we get

$$\sigma = \frac{\eta_0\dot{\gamma}_0}{1 + \tau^2\dot{\gamma}_0^2}, \quad \eta = \frac{\eta_0}{1 + \tau^2\dot{\gamma}_0^2}. \quad (4.14)$$

Under pure oscillating shear flow  $\dot{\gamma}(t) = \alpha\dot{\gamma}_0 e^{i\omega t}$ , we get

$$\sigma(t) = \frac{\alpha\eta_0\dot{\gamma}_0 e^{i\omega t}}{1 + i\omega\tau}, \quad \eta(\omega) = \frac{\eta_0}{1 + i\omega\tau}. \quad (4.15)$$

Under combined steady and oscillating shear flows  $\dot{\gamma}(t) = \dot{\gamma}_0(1 + \alpha e^{i\omega t})$ , we get

$$\sigma(t) = \frac{\eta_0\dot{\gamma}_0}{1 + \tau^2\dot{\gamma}_0^2} \left( 1 + \alpha \frac{1 + i\omega\tau - \tau^2\dot{\gamma}_0^2}{[1 + i\tau(\omega + \dot{\gamma}_0)][1 + i\tau(\omega - \dot{\gamma}_0)]} e^{i\omega t} \right), \quad (4.16)$$

$$\eta(t) = \frac{\eta_0}{1 + \tau^2\dot{\gamma}_0^2} \left( 1 + \alpha \frac{-i\omega\tau + \omega^2\tau^2 - 2\tau^2\dot{\gamma}_0^2}{[1 + i\tau(\omega + \dot{\gamma}_0)][1 + i\tau(\omega - \dot{\gamma}_0)]} e^{i\omega t} \right), \quad (4.17)$$

$$\eta_1(\omega) = \frac{\eta_0}{1 + \tau^2\dot{\gamma}_0^2} \frac{-i\omega\tau + \omega^2\tau^2 - 2\tau^2\dot{\gamma}_0^2}{[1 + i\tau(\omega + \dot{\gamma}_0)][1 + i\tau(\omega - \dot{\gamma}_0)]}. \quad (4.18)$$

One can check that there is a resonance in the spectrum (4.18) located close to the constant part of the shear rate  $\dot{\gamma}_0$ . Therefore, this model shows different responses to oscillating shear rate (1.1) and to oscillations (1.2) imposed on top of steady shear flow. We see that the spectra for TT vesicles in both relaxation regimes (OD and UD; see figures 2 and 3) can be reproduced by a macroscopic constitutive equation. It is not clear whether there is such a macroscopic constitutive law for a suspension of VB/TB vesicles that reproduces the spectra on figures 4 and 5. It will be an interesting task for future investigation to consider this question in detail.

The reported results on the complex viscosity are not devoid of experimental testability. Recent experiments on suspension of vesicles (Kantsler *et al.* 2008; Vitkova *et al.* 2008) and RBCs (Vitkova *et al.* 2008) under a constant shear flow agree with the behaviour of the viscosity as a function of the viscosity contrast (excluding the case of viscosity contrast less than 1, for which there is no agreement between experimental observations by Kantsler *et al.* (2008) and Vitkova *et al.* (2008)). However, the studies using small oscillations of the shear rate are much more demanding to the precision of the rheometer: it is necessary to extract correctly a small oscillating signal from the main constant (yet noisy) background. Another limitation comes from the fact that

vesicles in suspensions have different values of capillary number (due to difference in size) and excess area. Thus dilute suspensions of RBCs, which are naturally much more homogeneous, are more promising targets for rheological studies under combined steady and oscillating shear flows.

Finally, let us emphasize that the main outcome of the present analysis does not depend on the precise form of the evolution equations. The spectra for the complex viscosity reported here should arise in any other situation where the suspended entities exhibit damped oscillations or periodic motions under constant shear rate. Known examples of this categories are, in addition to vesicles, capsules and RBCs.

### Acknowledgement

We acknowledge financial support from CNES and the ANR ‘MOSICOB project’.

### Appendix A. Shape evolution equations

The evolution equation derived in Danker *et al.* (2007) (equation (52) of [3]) can be written in a compact form as

$$\frac{\mathcal{D}\mathbf{F}}{\mathcal{D}t} = \lambda_1 \mathbf{e} + \lambda_2 (Z_0 + 6\kappa) \mathbf{F} + \lambda_3 Sd(\mathbf{F} \cdot \mathbf{e}) + (\lambda_4 Z_0 + \lambda_5 \kappa) Sd(\mathbf{F} \cdot \mathbf{F}) \quad (\text{A } 1)$$

with

$$Z_0 = - \frac{\lambda_1 \mathbf{F} \cdot \mathbf{e} + \bar{\lambda}_2 \kappa + \lambda_3 \mathbf{F} : (\mathbf{F} \cdot \mathbf{e}) + \lambda_5 \kappa \mathbf{F} : (\mathbf{F} \cdot \mathbf{F})}{\bar{\lambda}_2 + \lambda_4 \mathbf{F} : (\mathbf{F} \cdot \mathbf{F})} \quad (\text{A } 2)$$

where we have adopted the abbreviation  $Sd[b_{ij}] = 1/2[b_{ij} + b_{ji} - (2/3)\delta_{ij}b_{ll}]$  and set

$$\lambda_1 = \frac{20}{\Lambda \sqrt{\Delta}}, \quad \Lambda = 23\lambda + 32, \quad \lambda_2 = -\frac{24\kappa}{\Lambda}, \quad \lambda_3 = \frac{4800(\lambda - 2)}{\Lambda^2} \quad (\text{A } 3)$$

$$\left. \begin{aligned} \lambda_4 &= \frac{288\sqrt{\Delta}(49\lambda + 136)}{\Lambda^2}, & \lambda_5 &= \frac{41472\sqrt{\Delta}(3\lambda + 7)}{7\Lambda^2}, \\ \bar{\lambda}_2 &= \frac{5\lambda_2}{32\pi}, & \bar{\lambda}'_2 &= \frac{5\lambda_2}{192\pi}, \end{aligned} \right\} \quad (\text{A } 4)$$

and

$$\mathbf{e} = \frac{\nabla \otimes \mathbf{V} + (\nabla \otimes \mathbf{V})^T}{2}. \quad (\text{A } 5)$$

The application of the Jaumann (or corotational) derivative  $\mathcal{D}/\mathcal{D}t$  on a tensor  $\mathbf{M}$  is defined by

$$\frac{\mathcal{D}\mathbf{M}}{\mathcal{D}t} = \frac{1}{2}[\mathbf{M}_{(1)} + \mathbf{M}^{(1)}], \quad (\text{A } 6)$$

where  $\mathbf{M}_{(1)}$  and  $\mathbf{M}^{(1)}$  are the upper and lower convected derivatives (known also as the contravariant and covariant derivatives, respectively), and are defined as

$$\mathbf{M}_{(1)} = \frac{\mathcal{D}\mathbf{M}}{\mathcal{D}t} - \mathbf{M} \cdot (\nabla \otimes \mathbf{V}) - (\nabla \otimes \mathbf{V})^T \cdot \mathbf{M} \quad (\text{A } 7a)$$

$$\mathbf{M}^{(1)} = \frac{\mathcal{D}\mathbf{M}}{\mathcal{D}t} + (\nabla \otimes \mathbf{V}) \cdot \mathbf{M} + \mathbf{M} \cdot (\nabla \otimes \mathbf{V})^T, \quad (\text{A } 7b)$$

where  $\mathcal{D}\mathbf{M}/\mathcal{D}t$  is the usual material derivative (equal to  $\dot{\mathbf{M}}$  in our case).



**Appendix B. The average stress tensor**

The stress produced by a particle  $\sigma_{ij}$  in (1.9) is calculated from the Batchelor formula (Batchelor 1970):

$$\sigma_{ij} = \int [f_i^m x_j + (\eta_{int} - \eta_{ext})(n_i v_j + v_i n_j)] dA, \tag{B 1}$$

where  $f^m$  is the force exerted by the vesicle membrane on surrounding fluids,  $n$  is the normal vector and  $dA$  is the surface area element. Using the solution provided in (Danker *et al.* 2007), the stress tensor as a function of the vesicle conformation can be calculated. It is found to be

$$\begin{aligned} \frac{\sigma}{3\eta_{ext}} &= \frac{5}{3} \frac{23\lambda - 16}{23\lambda + 32} \mathbf{e} + \frac{96}{23\lambda + 32} \sqrt{\Delta} (Z_0 + 6\kappa) \mathbf{F} \\ &+ \sqrt{\Delta} \frac{5}{14(23\lambda + 32)^2} (529\lambda^2 - 1008\lambda - 256) Sd(\mathbf{F} \cdot \mathbf{e}) \\ &- \Delta \frac{192}{7(23\lambda + 32)^2} [(1056 + 174\lambda)\kappa + (112 - 17\lambda)Z_0] Sd(\mathbf{F} \cdot \mathbf{F}). \end{aligned} \tag{B 2}$$

**Appendix C. Discussion of the divergence of  $\eta_1$  in VB/TB phases**

Here we discuss why the complex viscosity for VB/TB vesicles remains bounded in the vicinity of a resonance frequency for a given amplitude of the imposed oscillations. As was discussed, the divergence of  $\eta_1(\omega)$  in the linear response approximation in VB/TB phases is related to the excitation of oscillations of the offset of the phase of VB/TB motion. To study this problem, we use the following ansatz:

$$F_{i,j}(t) = F_{i,j}^{(0)}(t') + \alpha \xi_2(t') e^{v t'} \varphi_{i,j}(t'), \tag{C 1}$$

where  $v$  and  $\varphi_{i,j}$  are the same as used in (3.5). The difference from the ansatz (3.5) is that we use effective time  $t'$  instead of the actual time  $t$  to absorb the term diverging in linear response approximation. The difference,  $\delta t(t') = t' - t$  reflects the drift of the phase of VB/TB motion under the effect of the imposed oscillations and no assumption about its smallness will be made. Nevertheless, the time derivative of  $\delta t$  is proportional to the amplitude of the imposed oscillations and thus will be considered to have smallness  $O(\alpha)$ . Taking the time derivative of (C 1), we get

$$\begin{aligned} \frac{dF_{i,j}(t)}{dt} &= \frac{dF_{i,j}^{(0)}(t')}{dt'} \left( 1 + \frac{d\delta t(t')}{dt} \right) + \alpha \frac{d(\xi_2(t') e^{v t'} \varphi_{i,j}(t'))}{dt} \\ &= \frac{dF_{i,j}^{(0)}(t')}{dt'} \left( 1 + \frac{d\delta t(t')}{dt'} \right) + \alpha \frac{d(\xi_2(t') e^{v t'} \varphi_{i,j}(t'))}{dt'} + O(\alpha^2), \end{aligned} \tag{C 2}$$

where we used that  $dt'/dt = 1 + O(\alpha)$ . Now we substitute (C 1) into the right-hand side of (1.7):

$$\begin{aligned} f_{i,j}(F_{i',j'}(t)) &= f_{i,j}(F_{i',j'}^{(0)}(t'), \dot{\gamma}_0) + \alpha \frac{\partial f_{i,j}}{\partial F_{i',j'}}(t') \xi_2(t') e^{v t'} \varphi_{i',j'}(t') \\ &+ \alpha \dot{\gamma}_0 \frac{\partial f_{i,j}}{\partial \dot{\gamma}}(t') e^{i\omega t} + O(\alpha^2). \end{aligned} \tag{C 3}$$

All of the partial derivatives are evaluated for unperturbed motion but at the time  $t'$ . Equating (C2) and (C3), we see that the  $O(1)$  terms cancel out. At order  $O(\alpha)$  we get

$$\frac{1}{\alpha} \frac{d\delta t(t')}{dt'} \frac{F_{ij}^{(0)}(t')}{dt'} + \frac{d\xi_2(t')}{dt'} e^{vt'} \varphi_{i,j}(t') = \dot{\gamma}_0 \frac{\partial f_{i,j}}{\partial \dot{\gamma}}(t') e^{i\omega t} = \dot{\gamma}_0 \frac{\partial \tilde{f}_{i,j}}{\partial \dot{\gamma}}(t') e^{i\omega(t' - \delta t(t'))}, \quad (C4)$$

where we have used the fact that  $e^{vt'} \varphi_{i,j}(t')$  is a solution of the homogeneous equation (3.1). Now we remember the decomposition (3.7), which allows us to separate the equations of  $\delta t$  and  $\xi_2$ :

$$\frac{1}{\alpha} \frac{d\delta t(t')}{dt'} = \dot{\gamma}_0 G_1(t') e^{i\omega(t' - \delta t(t'))}, \quad (C5)$$

$$\frac{d\xi_2(t')}{dt'} = \dot{\gamma}_0 G_2(t') e^{-vt' - i\omega(t' - \delta t(t'))}. \quad (C6)$$

Since these equations have a solution, our initial ansatz (C1) is justified. Equation (C5) can actually be integrated:

$$e^{i\omega \delta t(t')} = e^{i\omega \xi_1^{(0)}} + \alpha \dot{\gamma}_0 \int_0^{t'} G_1(\tau) e^{i\omega \tau} d\tau \quad (C7)$$

but, since we are not interested in the computation of  $\eta_1(\omega)$  in the general case, we will not use this solution. Instead, we substitute the ansatz (C1) into the expression for the stress of the suspension (1.10):

$$\sigma_{xy}(t) = \sigma_{xy}(t') + \alpha \frac{\partial \sigma_{xy}}{\partial F_{ij}}(t') \xi_2(t') e^{vt'} \varphi_{i,j}(t') + \alpha \dot{\gamma}_0 \frac{\partial \sigma_{xy}}{\partial \dot{\gamma}}(t') e^{i\omega t} + O(\alpha^2) \quad (C8)$$

and use the straightforward definition to calculate  $\sigma_{xy}(\omega)$ :

$$\sigma_{xy}(\omega) = \lim_{t_0 \rightarrow \infty} \frac{1}{t_0} \int_0^{t_0} \sigma_{xy}(t) e^{-i\omega t} dt. \quad (C9)$$

The terms, diverging in the linear response approximation, are now combined into the  $\sigma_{xy}(t')$  term. Nevertheless, we shall also prove that  $O(\alpha)$  terms remain bounded. The proof is straightforward

$$\begin{aligned} |\sigma_{xy}(\omega)| &= \lim_{t_0 \rightarrow \infty} \frac{1}{t_0} \left| \int_0^{t_0} \sigma_{xy}(t) e^{-i\omega t} dt \right| \leq \lim_{t_0 \rightarrow \infty} \frac{1}{t_0} \int_0^{t_0} |\sigma_{xy}(t)| dt \\ &= \lim_{t_0 \rightarrow \infty} \frac{1}{t_0} \int_0^{t_0} \left| \sigma_{xy}(t') + \alpha \frac{\partial \sigma_{xy}}{\partial F_{ij}}(t') \xi_2(t') e^{vt'} \varphi_{i,j}(t') + \alpha \dot{\gamma}_0 \frac{\partial \sigma_{xy}}{\partial \dot{\gamma}}(t') e^{i\omega t} \right| dt \\ &\leq \lim_{t_0 \rightarrow \infty} \frac{1}{t_0} \int_0^{t_0} \left[ |\sigma_{xy}(t')| + \alpha \left| \frac{\partial \sigma_{xy}}{\partial F_{ij}}(t') \xi_2(t') e^{vt'} \varphi_{i,j}(t') \right| + \alpha \dot{\gamma}_0 \left| \frac{\partial \sigma_{xy}}{\partial \dot{\gamma}}(t') \right| \right] dt \\ &\leq \max_{0 \leq t < T} |\sigma^{(0)}(t)| + \alpha \dot{\gamma}_0 \lim_{t_0 \rightarrow \infty} \frac{1}{t_0} \int_0^{t_0} \left| \frac{\partial \sigma_{xy}}{\partial F_{ij}}(t') \xi_2(t') e^{vt'} \varphi_{i,j}(t') \right| dt \\ &\quad + \alpha \dot{\gamma}_0 \max_{0 \leq t < T} \left| \frac{\partial \sigma_{xy}^{(0)}(t)}{\partial \dot{\gamma}} \right|. \end{aligned} \quad (C10)$$

The first and the third terms are clearly bounded because of the continuity of  $\sigma^{(0)}$  and its derivative, the second term can be evaluated using (C 6):

$$\begin{aligned} \left| \frac{\partial \sigma_{xy}}{\partial F_{ij}}(t') \xi_2(t') e^{vt'} \varphi_{ij}(t') \right| &= \left| \frac{\partial \sigma_{xy}}{\partial F_{ij}}(t') \left[ \xi_2^{(0)} + \int_0^{t'} G_2(\tau) e^{-v\tau - i\omega(\tau' - \delta t(\tau'))} d\tau \right] e^{vt'} \varphi_{ij}(t') \right| \\ &\leq \left| \frac{\partial \sigma_{xy}}{\partial F_{ij}}(t') \varphi_{ij}(t') \right| \left[ |\xi_2^{(0)}| + \int_0^{t'} |G_2(\tau)| e^{v(t' - \tau)} d\tau \right] \\ &\leq \max_{0 \leq t < T} \left| \frac{\partial \sigma_{xy}}{\partial F_{ij}}(t) \varphi_{ij}(t) \right| \left[ |\xi_2^{(0)}| + \frac{1}{|v|} \max_{0 \leq \tau < T} |G_2(\tau)| \right]. \quad (\text{C } 11) \end{aligned}$$

This expression and, consequently, its average over long time is bounded, which proves that oscillations of the stress in the suspension are finite but can become large even for very small amplitude of the oscillations of the imposed shear rate.

Finally, the amplitude of the oscillations of  $\delta t(t')$  is proportional to  $\alpha/\delta\omega$ , where  $\delta\omega = \min_k |\omega - k\Omega|$  is the difference between the frequency of the imposed oscillations and the nearest integer multiple of the VB/TB frequency. We have to demand that  $\alpha/\delta\omega$  be small if we want the linear response approximation and the expansion (1.11) to be valid.

#### REFERENCES

- BAGCHI, P. & KALLURI, R. M. 2009 Dynamics of nonspherical capsules in shear flow. *Phys. Rev. E* **80** (1), 016307.
- BAGCHI, P. & KALLURI, R. M. 2011 Dynamic rheology of a dilute suspension of elastic capsules: effect of capsule tank-treading, swinging and tumbling. *J. Fluid Mech.* **669**, 498–526.
- BARTHÈS-BIESEL, D. 2009 Capsule motion in flow: Deformation and membrane buckling. *Comptes Rendus Physique* **10** (8), 764–774.
- BATCHELOR, G. K. 1970 The stress system in a suspension of force-free particles. *J. Fluid Mech.* **41** (03), 545–570.
- BIBEN, T., FARUTIN, A. & MISBAH, C. 2011 Three-dimensional vesicles under shear flow: Numerical study of dynamics and phase diagram. *Phys. Rev. E* **83** (3), 031921.
- BIRD, R. B., ARMSTRONG, R. C. & HASSAGER, O. 1987 *Dynamics of Polymeric Liquids*, 2nd edn. *Fluid Dynamics*, vol. 1. Wiley.
- BOOIJ, H. C. 1966a Influence of superimposed steady shear flow on the dynamic properties of non-Newtonian fluids. I. Measurements on non-Newtonian solutions. *Rheol. Acta* **5**, 215–221.
- BOOIJ, H. C. 1966b Influence of superimposed steady shear flow on the dynamic properties of non-Newtonian fluids. II. Theoretical approach based on the Oldroyd theory. *Rheol. Acta* **5**, 222–227.
- CLAUSEN, J. R. & AIDUN, C. K. 2010 Capsule dynamics and rheology in shear flow: Particle pressure and normal stress. *Phys. Fluids* **22** (12), 123302.
- COX, R. G. 1969 The deformation of a drop in a general time-dependent fluid flow. *J. Fluid Mech.* **37** (03), 601–623.
- DANKER, G., BIBEN, T., PODGORSKI, T., VERDIER, C. & MISBAH, C. 2007 Dynamics and rheology of a dilute suspension of vesicles: Higher-order theory. *Phys. Rev. E* **76** (4), 041905.
- DANKER, G. & MISBAH, C. 2007 Rheology of a dilute suspension of vesicles. *Phys. Rev. Lett.* **98** (8), 088104.
- DESCHAMPS, J., KANTSLER, V. & STEINBERG, V. 2009 Phase diagram of single vesicle dynamical states in shear flow. *Phys. Rev. Lett.* **102** (11), 118105.
- FARUTIN, A., BIBEN, T. & MISBAH, C. 2010 Analytical progress in the theory of vesicles under linear flow. *Phys. Rev. E* **81** (6), 061904.

- FRANKEL, N. A. & ACRIVOS, A. 1970 The constitutive equation for a dilute emulsion. *J. Fluid Mech.* **44** (01), 65–78.
- GHIGLIOTTI, G., BIBEN, T. & MISBAH, C. 2010 Rheology of a dilute two-dimensional suspension of vesicles. *J. Fluid Mech.* **653**, 489–518.
- KANTSLEER, V., SEGRE, E. & STEINBERG, V. 2008 Dynamics of interacting vesicles and rheology of vesicle suspension in shear flow. *Europhys. Lett.* **82** (5), 58005.
- KANTSLEER, V. & STEINBERG, V. 2006 Transition to tumbling and two regimes of tumbling motion of a vesicle in shear flow. *Phys. Rev. Lett.* **96**, 036001.
- LARSON, R. G. 1999 *The Structure and Rheology of Complex Fluids*. Oxford University Press.
- LEBEDEV, V. V., TURITSYN, K. S. & VERGELES, S. S. 2007 Dynamics of nearly spherical vesicles in an external flow. *Phys. Rev. Lett.* **99** (21), 218101.
- LEBEDEV, V. V., TURITSYN, K. S. & VERGELES, S. S. 2008 Nearly spherical vesicles in an external flow. *New J. Phys.* **10** (4), 043044.
- MISBAH, C. 2006 Vacillating breathing and tumbling of vesicles under shear flow. *Phys. Rev. Lett.* **96** (2), 028104.
- NOGUCHI, H. & GOMPPER, G. 2007 Swinging and tumbling of fluid vesicles in shear flow. *Phys. Rev. Lett.* **98** (12), 128103.
- TIRTAATMADJA, V., TAM, K. C. & JENKINS, R. D. 1997 Superposition of oscillations on steady shear flow as a technique for investigating the structure of associative polymers. *Macromolecules* **30** (5), 1426–1433.
- VERGELES, S. 2008 Rheological properties of a vesicle suspension. *JETP Lett* **87**, 511–515.
- VITKOVA, V., MADER, M.-A., POLACK, B., MISBAH, C. & PODGORSKI, T. 2008 Micro-macro link in rheology of erythrocyte and vesicle suspensions. *Biophys. J* **95** (6), L33–L35.
- VLAHOVSKA, P. M. & GRACIA, R. S. 2007 Dynamics of a viscous vesicle in linear flows. *Phys. Rev. E* **75** (1), 016313.
- VLAHOVSKA, P. M., PODGORSKI, T. & MISBAH, C. 2009 Vesicles and red blood cells in flow: From individual dynamics to rheology. *Comptes Rendus Physique* **10** (8), 775–789.
- VLASTOS, G., LERCHE, D., KOCH, B., SAMBA, O. & POHL, M. 1997 The effect of parallel combined steady and oscillatory shear flows on blood and polymer solutions. *Rheol. Acta* **36**, 160–172.
- YAZDANI, A. Z. K., KALLURI, R. M. & BAGCHI, P. 2011 Tank-treading and tumbling frequencies of capsules and red blood cells. *Phys. Rev. E* **83** (4), 046305.
- ZHAO, H. & SHAQFEH, E. S. G. 2011 The dynamics of a vesicle in simple shear flow. *J. Fluid Mech.* **674**, 578–604.